

UC Irvine

UC Irvine Previously Published Works

Title

N-(2-Oxo-3-oxetanyl)carbamic Acid Esters as N-Acylethanolamine Acid Amidase Inhibitors: Synthesis and Structure-Activity and Structure-Property Relationships

Permalink

<https://escholarship.org/uc/item/8282x958>

Journal

Journal of Medicinal Chemistry, 55(10)

ISSN

0022-2623

Authors

Duranti, Andrea
Tontini, Andrea
Antonietti, Francesca
et al.

Publication Date

2012-05-24

DOI

10.1021/jm300349j

Copyright Information

This work is made available under the terms of a Creative Commons Attribution License, available at <https://creativecommons.org/licenses/by/4.0/>

Peer reviewed

N-(2-Oxo-3-oxetanyl)carbamic Acid Esters as *N*-Acylethanolamine Acid Amidase Inhibitors: Synthesis and Structure–Activity and Structure–Property Relationships

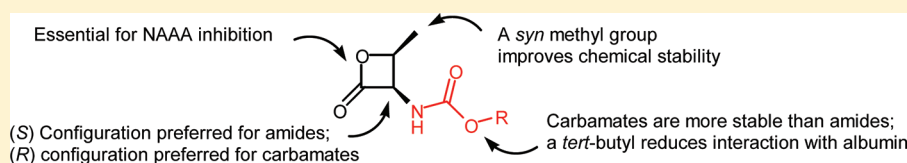
Andrea Duranti,[†] Andrea Tontini,[†] Francesca Antonietti,[†] Federica Vacondio,[‡] Alessandro Fioni,[‡] Claudia Silva,[‡] Alessio Lodola,[‡] Silvia Rivara,[‡] Carlos Solorzano,[§] Daniele Piomelli,^{§,||} Giorgio Tarzia,[†] and Marco Mor*[‡]

[†]Dipartimento di Scienze Biomolecolari, Università degli Studi di Urbino “Carlo Bo”, Piazza del Rinascimento 6, I-61029 Urbino, Italy

[‡]Dipartimento Farmaceutico, Università degli Studi di Parma, Viale G. P. Usberti 27/A, I-43124 Parma, Italy

[§]Department of Pharmacology, University of California, Irvine, 360 MSRII, California 92697-4625, United States

^{||}Department of Drug Discovery and Development, Italian Institute of Technology, via Morego 30, I-16163 Genova, Italy



ABSTRACT: The β -lactone ring of *N*-(2-oxo-3-oxetanyl)amides, a class of *N*-acylethanolamine acid amidase (NAAA) inhibitors endowed with anti-inflammatory properties, is responsible for both NAAA inhibition and low compound stability. Here, we investigate the structure–activity and structure–property relationships for a set of known and new β -lactone derivatives, focusing on the new class of *N*-(2-oxo-3-oxetanyl)carbamates. Replacement of the amide group with a carbamate one led to different stereoselectivity for NAAA inhibition and higher intrinsic stability, because of the reduced level of intramolecular attack at the lactone ring. The introduction of a *syn* methyl at the β -position of the lactone further improved chemical stability. A *tert*-butyl substituent in the side chain reduced the reactivity with bovine serum albumin. (2*S*,3*R*)-2-Methyl-4-oxo-3-oxetanylcarbamic acid 5-phenylpentyl ester (**27**, URB913/ARN077) inhibited NAAA with good in vitro potency ($IC_{50} = 127$ nM) and showed improved stability. It is rapidly cleaved in plasma, which supports its use for topical applications.

■ INTRODUCTION

Fatty acid ethanolamides (FAEs) make up a family of bioactive mediators that have stimulated pharmaceutical interest because compounds blocking their deactivating hydrolysis offer a new strategy for the treatment of pain and inflammation.^{1–3} An endogenous FAE that has attracted considerable attention is palmitoylethanolamide (PEA),^{4,5} which has been found to modulate pain and inflammation by engaging peroxisome proliferator-activated receptor type α .^{6,7} In particular, PEA has been shown to inhibit peripheral inflammation and mast cell degranulation⁸ and to exert antinociceptive effects in rodent models of acute and chronic pain.⁹ PEA has also been found to suppress pain behaviors induced by tissue injury, nerve damage, or inflammation in mice.¹⁰

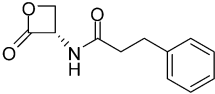
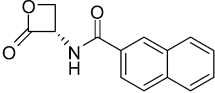
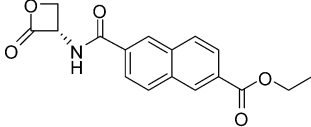
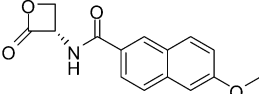
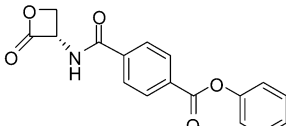
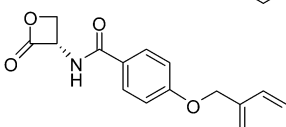
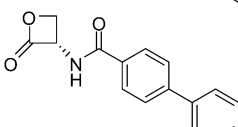
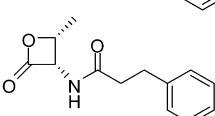
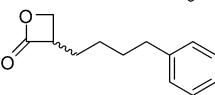
Along with PEA, other FAEs having neuromodulatory functions have been identified. These include the endogenous cannabinoid agonist *N*-arachidonylethanolamine (anandamide, AEA)¹¹ and the feeding regulator oleoylethanolamide.^{12,13} FAEs share similar anabolic and catabolic pathways, with their levels finely controlled by enzymes responsible for synthesis and degradation.¹⁴ FAEs are produced by the action of a selective phospholipase D, which catalyzes the cleavage of the membrane precursor *N*-acylphosphatidylethanolamine.^{15,16} The hydrolysis of anandamide is mostly attributed to fatty acid

amide hydrolase (FAAH),¹⁷ an intracellular membrane-bound protein belonging to the amidase signature (AS) family, characterized by an optimal activity at pH 9.0.¹⁸ On the other hand, PEA is primarily hydrolyzed by *N*-acylethanolamine acid amidase (NAAA),¹⁹ which is not related to FAAH or other members of the AS family, is localized in the lysosomes, and shows an optimal activity at pH 5.0.²⁰ NAAA is an N-terminal nucleophile hydrolase (Ntn) and belongs to the cholesterylglycine hydrolase family of hydrolases,²¹ which are characterized by the ability to cleave nonpeptide amide bonds. Like other Ntn enzymes, NAAA is converted by self-catalyzed proteolysis into a shorter active form upon incubation at acidic pH.²² Processing of NAAA renders a cysteine residue (Cys131 in rat NAAA and Cys126 in human NAAA) the N-terminal amino acid. Site-directed mutagenesis^{23,24} and mass spectrometry²⁵ studies demonstrated that this N-terminal cysteine plays a pivotal role in both catalytic activity and proteolytic processing. This is consistent with a catalytic mechanism involving the exchange of a proton between the sulfhydryl and the amino groups of the terminal cysteine and a nucleophile attack on the amide carbonyl of the substrate, as supported by quantum

Received: March 13, 2012

Published: April 19, 2012

Table 1. Stabilities of Compounds 1–9 in Buffers and in the Presence of Thiols

Cpds.	Structure	pH 7.4 $t_{1/2}$ (min)	pH 5.0 $t_{1/2}$ (min)	pH 5.0 + DTT $t_{1/2}$ (min)
1		18.0 ± 1.1	23.1 ± 0.8	19.0 ± 0.4
2		9.8 ± 0.8	19.0 ± 1.7	15.9 ± 2.0
3		12.1 ± 1.7	25.1 ± 2.3	20.9 ± 1.8
4		8.2 ± 2.6	18.1 ± 1.9	19.1 ± 2.0
5		9.8 ± 1.5	23.7 ± 2.0	19.5 ± 1.9
6		13.4 ± 2.0	23.2 ± 1.7	18.8 ± 2.2
7		12.6 ± 1.4	28.4 ± 1.7	20.9 ± 2.1
8		73.8 ± 1.6	134.6 ± 2.4	100.2 ± 2.7
9		93.5 ± 3.4	114.6 ± 3.9	113.8 ± 5.0

mechanics/molecular mechanics (QM/MM) simulations for cysteine Ntn hydrolases.²⁶

Recently, the level of interest in NAAA as a pharmaceutically relevant target has increased, because of the observation that NAAA inhibitors locally administered to inflamed tissues, where the biosynthesis of PEA is downregulated,⁷ restore the physiological levels of PEA.²⁴ While several classes of potent and selective FAAH inhibitors have been discovered and employed to study the central^{27,28} and peripheral²⁹ role of FAAH, only few NAAA inhibitors have been reported.^{24,30–32} To further investigate the usefulness of NAAA inhibitors in acute and chronic inflammation, the discovery of new potent and selective compounds and the optimization of known chemical classes are both needed.

In this context, our research group has recently identified a class of β -lactone-based NAAA inhibitors, exemplified by (*S*)-*N*-(2-oxo-3-oxetanyl)-3-phenylpropanamide [(*S*)-OOPP, **1** (Table 1)], which weakens responses to inflammatory stimuli by elevating PEA levels in vitro and in vivo,²⁴ and described the structure–activity relationships (SARs) of a series of *N*-(2-oxo-3-oxetanyl)amides.³³ These compounds inhibit NAAA with a rapid, noncompetitive, and reversible mechanism, consistent

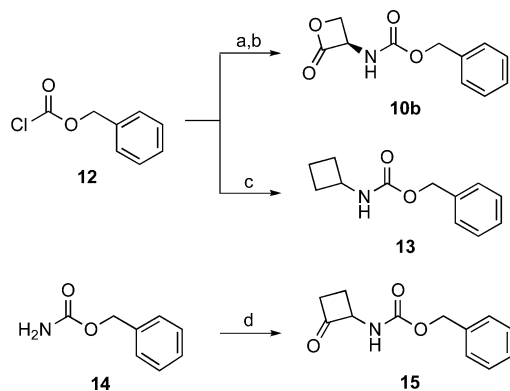
with the acylation of the catalytic Cys131. Among the synthesized *N*-(2-oxo-3-oxetanyl)amides, compound **7** (Table 1) had an IC_{50} of 115 nM and was effective at reducing the level of carrageenan-induced leukocyte infiltration in vivo.³³ The α -amino- β -lactone moiety, although essential for the inhibitory activity of *N*-(2-oxo-3-oxetanyl)amides, is responsible for the low chemical stability of these compounds. Indeed, compounds incorporating an α -amino- β -lactone portion promptly react with bionucleophiles³⁴ and are readily hydrolyzed in aqueous media.^{35,36} As a consequence, their use in pharmacological studies remains restricted to topical administration and requires caution in their handling and storage.

In this work, we investigated the mechanism of degradation of NAAA inhibitors with an α -amino- β -lactone scaffold, including the known *N*-(2-oxo-3-oxetanyl)amides, and expanded the series to new *N*-(2-oxo-3-oxetanyl)carbamic acid esters, which were designed and synthesized to explore the effect of the side chain on inhibitory activity and chemical stability. SARs and structure–property relationships (SPRs) demonstrated that the introduction of an α -carbamic acid ester side chain and a β -methyl group on the β -lactone ring resulted in potent NAAA inhibitors with enhanced chemical stability.

CHEMISTRY

Compounds 1–9 were obtained as reported elsewhere.³³ **10a** was prepared by a literature procedure.³⁶ *N*-Benzyloxycarbonyl-L-serine (*N*-Cbz-L-serine, **11a**) was purchased from Lancaster.

The β -lactone **10b**³⁷ and the cyclobutane derivative **13**³⁸ were synthesized starting from benzyl chloroformate (**12**) (Scheme 1). **12** was treated with cyclobutylamine, in the case of

Scheme 1^a

^aReagents and conditions: (a) D-serine, NaHCO₃, H₂O, THF, room temperature for 1 h; (b) PPh₃, DMAD, THF, –78 °C for 3 h, room temperature for 3 h; (c) *c*-C₄H₇NH₂, NaHCO₃, H₂O, room temperature for 3 h; (d) 1,2-bis(trimethylsilyloxy)cyclobutene, HCl/Et₂O, 0 °C and reflux for 4 h.

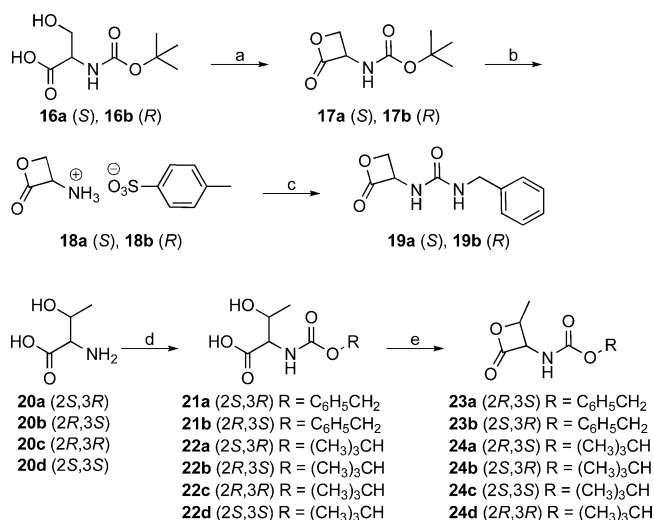
13, or D-serine, in aqueous sodium bicarbonate. In the latter case, the resulting intermediate *N*-Cbz-D-serine (**11b**) was cyclized to **10b** by means of a modified Mitsunobu reaction, employing dimethyl azodicarboxylate (DMAD) and dry triphenylphosphine.³⁶

Cyclobutanone derivative **15**³⁶ was synthesized by a reaction between benzyl carbamate (**14**) and 1,2-bis(trimethylsilyloxy)cyclobutene³⁹ in ethereal hydrogen chloride (Scheme 1).³⁶

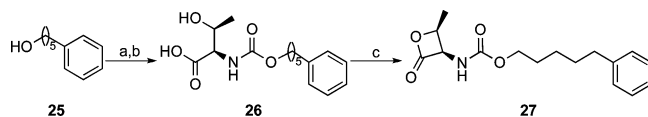
Ureas **19a** and **19b** were obtained by reacting benzyl isocyanate with (*S*)- and (*R*)-2-oxo-3-oxetanylammonium toluene-4-sulfonate (**18a**⁴⁰ and **18b**⁴¹), respectively, in turn synthesized by deprotection of β -lactone derivatives **17a**³⁷ and **17b**,⁴² respectively, with dry trifluoroacetic acid in the presence of dry *p*-toluenesulfonic acid (Scheme 2).^{40,41} Intermediates **17a** and **17b** were prepared starting from *N*-*tert*-butyloxycarbonyl-L-serine (*N*-Boc-L-serine, **16a**) and *N*-Boc-D-serine (**16b**), respectively, employing the same method used for **10b** (Scheme 2).³⁷

The synthesis of threonine β -lactones **23a**,⁴³ **23b**,⁴⁴ **24a**,⁴⁴ **24b**,³³ **24c**, and **24d** is illustrated in Scheme 2. The amino groups of L-, D-, L-*allo*-, and D-*allo*-threonine (**20a–d**, respectively) were protected with **12** or di-*tert*-butyl dicarbonate (Boc₂O) in aqueous sodium bicarbonate to give **21a**,⁴⁵ **21b**,⁴⁶ **22a**,⁴⁷ **22b**,⁴⁸ **22c**,⁴⁹ and **22d**,⁵⁰ respectively, employing a slightly modified literature procedure.⁵¹ Cyclization to β -lactones **23a,b** and **24a–d** was accomplished by treating the parent compounds **21a,b** and **22a–d**, respectively, with benzotriazol-1-yloxytris(dimethylamino)phosphonium hexafluorophosphate (BOP reagent) by means of a literature procedure.³⁶

D-Threonine β -lactone **27** was synthesized as reported in Scheme 3. Commercially available 5-phenylpentanol (**25**) was reacted with bis(trichloromethyl) carbonate in the presence of pyridine to give 5-phenylpentyl chloroformate according to a

Scheme 2^a

^aReagents and conditions: (a) PPh₃, DMAD, THF, –78 °C for 20 min, room temperature for 2.5 h; (b) CF₃COOH, *p*-TsOH, 0 °C for 10–15 min; (c) C₆H₅CH₂NCO, Et₃N, THF, 0 °C for 30 min, room temperature for 3 h; (d) CbzCl, NaHCO₃, H₂O, THF, room temperature for 1 h (**21a,b**), or Boc₂O, NaHCO₃, H₂O, MeOH, room temperature for 36 h (**22a–d**); (e) BOP, Et₃N, CH₂Cl₂, 0 °C for 1 h, room temperature for 2 h (**23a,b**), or BOP, Et₃N, CH₂Cl₂, room temperature for 3 h (**24a–d**).

Scheme 3^a

^aReagents and conditions: (a) (Cl₃CO)₂CO, pyridine, toluene, 0 °C for 2 h, room temperature for 90 h; (b) **20b**, NaHCO₃, H₂O, THF, (*n*-Bu)₄NBr, room temperature for 18 h; (c) HBTU, Et₃N, CH₂Cl₂, 0 °C for 3 h, room temperature for 6 h.

literature procedure;⁵² the latter was treated with **20b** and tetrabutylammonium bromide in aqueous sodium bicarbonate to afford **26**, which was cyclized by means of the 2-(1*H*-benzotriazol-1-yl)-1,1,3,3-tetramethylammonium hexafluorophosphate (HBTU) carboxylic acid activating agent to give **27**.

RESULTS AND DISCUSSION

Chemical Stability of *N*-(2-Oxo-3-oxetanyl)amides.

The chemical stabilities of the previously published *N*-(2-oxo-3-oxetanyl)amides **1–8** and compound **9** are summarized in Table 1. Those compounds revealed high susceptibility to chemical hydrolysis in buffered solution both at pH 7.4 (physiological pH) and at pH 5.0 (pH for the in vitro rat NAAA inhibitory assay). Both aliphatic (**1**) and aromatic (**2–7**) *N*-(2-oxo-3-oxetanyl)amides have half-lives (*t*_{1/2}) of ≤18 min at pH 7.4 and ≤28 min at pH 5.0. The presence of dithiothreitol (DTT) (3 mM) in the pH 5.0 buffer did not significantly affect half-life values, indicating that the β -lactones do not preferentially react with thiols and that hydrolysis is the main factor for their instability under the assay conditions. This result is also relevant for the interpretation of the in vitro tests, as DTT was added to NAAA samples to maintain the catalytic activity of the enzyme over time.

The introduction of different electron-withdrawing (3 or 5) or electron-donating (4 or 6) substituents at conjugated positions did not significantly modify the stability of arylamides 2–7, which showed similar half-lives. Conversely, the introduction of a *syn* methyl group at position 4 (compound 8) led to a significant improvement in half-life, which was approximately 5-fold longer.

An investigation, performed by HPLC–ultraviolet (UV)–mass spectrometry (MS) analysis, of degradation products of amides 1–8 showed, at pH 7.4 and 5.0, the formation of *N*-acylated L-serines, which resulted from the hydrolytic opening of the β -lactone ring (data not shown). An important difference in stability was observed between amides 1–7 and alkyl lactone 9, which was significantly more stable with half-lives passing from 8.2–18.0 to 93.5 min at pH 7.4 and from 18.1–28.4 to 114.6 min at pH 5.0. Thus, the amide group of the side chain plays a role in the chemical degradation of the lactone ring.

Taking compound 2 as the representative of compounds 1–8, we conducted HPLC–UV–MS analysis at pH 7.4 and 5.0 of its hydrolysis time course and that of formation of the resulting products (Figure 1).

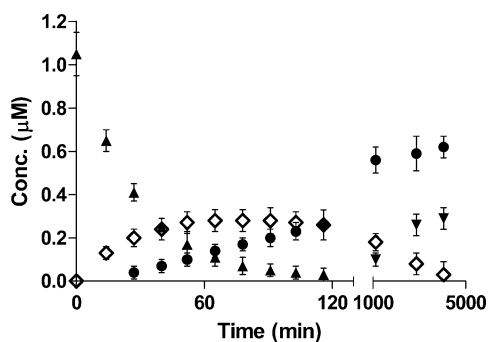


Figure 1. Time courses of the degradation products of compound 2 at pH 5.0: (▲) compound 2, (◇) *N*-(2-naphthoyl)-L-serine, (●) *O*-(2-naphthoyl)-L-serine, and (▼) 2-naphthoic acid.

N-(2-Naphthoyl)-L-serine was detected at pH 7.4, and its identity was confirmed by its m/z value ($[M - H]^- = 258.1$) and superposition of its HPLC peak with that of a standard sample. The hydrolysis of the amide side chain was significantly slower, as measurable amounts of 2-naphthoic acid were detected after only 24 h. At pH 5.0, a degradation product not observed at pH 7.4 was detected. The compound showed a retention time on a C_{18} RP column shorter than that of *N*-(2-naphthoyl)-L-serine and had an m/z value corresponding to the addition of a water molecule to compound 2 ($[M + H]^+ = 260.1$). The compound was identified as *O*-(2-naphthoyl)-L-

serine on the basis of its retention time and that of one authentic sample.

Figure 1 shows the time course and degradation products of 2 at pH 5.0. At time ≤ 2 h, 2 was converted rapidly into *N*-(2-naphthoyl)-L-serine [product A (Figure 2)] and more slowly into *O*-(2-naphthoyl)-L-serine [product B (Figure 2)]. At 2 h, no starting compound or 2-naphthoic acid [product C (Figure 2)] was detected, and approximately equal amounts of A and B were present, accounting together for $\sim 60\%$ of the total mass balance. At early time points, a peak with an m/z value corresponding to that of compound 2 ($[M - H]^- = 240.1$) was also observed, corresponding to an additional degradation product [D (Figure 2)]. At longer time points, the slow decrease in the level of *N*-(2-naphthoyl)-L-serine (product A) was paralleled by a corresponding increase in the level of 2-naphthoic acid. After 3 days, the sum of molar concentrations for compounds A–C, measured through calibration curves with pure standards, was more than 90% of the starting concentration of compound 2, and the peak of the additional degradation product (D) disappeared, probably because it converted into compound A or B. We hypothesized a degradation scheme for 2 involving an active role for the amide group, following what had been already proposed for the degradation of serine lactones in a different context (Figure 2).³³ In particular, a nucleophilic attack from the amide carbonyl to the β -methylene group of *N*-(2-oxo-3-oxetanyl)-amides would give the intermediate 5-dihydro-2-(2-naphthalenyl)-4-oxazolecarboxylic acid, having an m/z value consistent with product D, which would quickly be hydrolyzed to *O*-acylated amino acid B. At the same time, water could directly attack the lactone carbonyl of 2, giving *N*-acylated amino acid A. In fact, the time courses of starting lactone 2 and products A and B (Figure 1) suggest two simultaneous pathways: one involving hydrolysis of the lactone to give *N*-(2-naphthoyl)-L-serine (A) and the second yielding *O*-(2-naphthoyl)-L-serine (B) through the formation of oxazoline–carboxylic acid intermediate D, which could not be isolated or quantified but showed intense peaks in chromatograms at short time points (Figure 3). This interpretation is further supported by the experimental observation that *N*-(2-naphthoyl)-L-serine did not directly convert to *O*-(2-naphthoyl)-L-serine but was slowly hydrolyzed to 2-naphthoic acid when maintained at pH 5.0 for 3 days. *O*-(2-Naphthoyl)-L-serine was found to be stable at pH 5.0, whereas at pH 7.4, it was converted to *N*-(2-naphthoyl)-L-serine ($t_{1/2} \sim 280$ min).

As the only substitution that improved the chemical stability of the *N*-(2-oxo-3-oxetanyl)amides (i.e., the introduction of the methyl group at the β -position of the lactone) had shown a detrimental effect on rat NAAA inhibitory potency,³³ our attempt to optimize both potency and stability focused on the

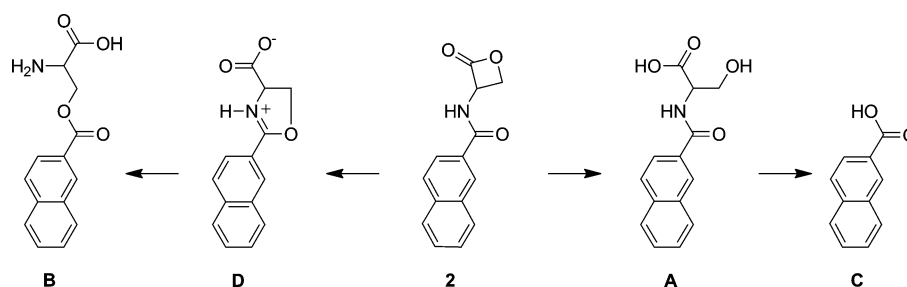


Figure 2. Possible routes of formation of *O*- and *N*-(2-naphthoyl)-L-serine from compound 2.

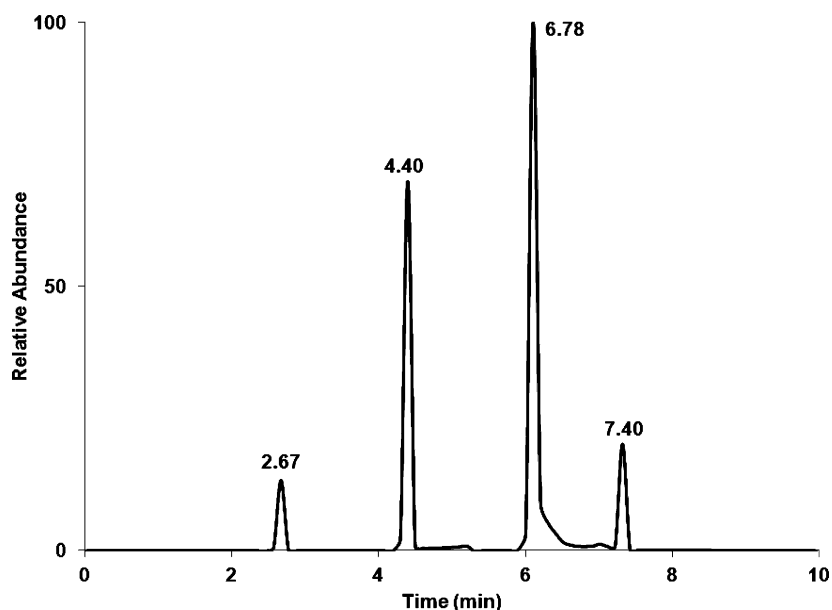


Figure 3. HPLC–MS chromatogram of compound 2 and its degradation products at pH 5.0 and 60 min, resulting from merging of selected ion chromatograms at m/z 240.1, 258.1, and 260.1. For *O*-(2-naphthoyl)-L-serine (B, $[M + H]^+ = 260.09$), $t_R = 2.67$ min. For *N*-(2-naphthoyl)-L-serine (A, $[M - H]^- = 258.09$), $t_R = 4.40$ min. For degradation product D ($[M - H]^- = 240.08$), $t_R = 6.78$ min. For compound 2 ($[M - H]^- = 240.08$), $t_R = 7.40$ min.

class of *N*-(2-oxo-3-oxetanyl)carbamic acid esters (Table 2), assuming that the lower nucleophilicity of the carbamate carbonyl would weaken the negative effect of the side chain on lactone stability. This hypothesis was based on quantum mechanical calculations for the internal nucleophilic attack on the β -carbon of the lactone ring by the side chain acyl oxygen, simulated for the two model compounds *N*-(2-oxo-3-oxetanyl)-acetamide and *N*-(2-oxo-3-oxetanyl)carbamic acid ester. Potential energy paths, calculated at the density functional theory (DFT) level (see Experimental Section for details), revealed that the carbamate has a higher potential energy barrier for oxazoline formation, probably because of the lower nucleophilicity of the carbamate carbonyl, compared to that of the carboxamide (Figure 4). The lower susceptibility of the carbamic acid ester to undergo internal cleavage was also confirmed by chemical stability data (e.g., carbamic acid esters **10a** and **23b**), which showed a significantly higher stability with respect to the corresponding amides **1** and **8**, the half-life going at pH 7.4 from 18.0–73.8 to 26.7–107.7 min and at pH 5.0 from 23.1–134.6 to 39.2–185.1 min. To improve the potency, we started a SAR exploration of *N*-(2-oxo-3-oxetanyl)carbamic acid esters. SPR analysis was also conducted to investigate the stereoelectronic requirements of the substituents at the α - and β -positions of the α -amino- β -lactone and the role of the size and shape of the carbamic acid ester side chain.

SAR of *N*-(2-Oxo-3-oxetanyl)carbamic Acid Esters. In our previous SAR exploration of *N*-(2-oxo-3-oxetanyl)amides, enantiomers with the (*S*) configuration at position 3 led to a 10-fold increase in rat NAAA inhibitory potency, compared to that of (*R*) compounds. This trend is reversed in the present *N*-(2-oxo-3-oxetanyl)carbamic acid esters, as the (*R*) analogue (**10b**) became more potent than its (*S*) enantiomer (**10a**), with IC_{50} values of 0.70 and 2.96 μM , respectively. As observed with *N*-(2-oxo-3-oxetanyl)amides, the essential role played in rat NAAA inhibitory potency by the intact β -lactone ring was confirmed by the lack of potency of open derivatives **11a** and **11b**, the cyclobutane, and cyclobutanone derivatives **13** and **15**

($IC_{50} > 100 \mu M$). Replacing the carbamate group with a urea, as in derivatives **19a** and **19b**, resulted in a marked decrease in potency (IC_{50} values of 15 and 49 μM , respectively). Two further structural modifications were attempted. First, we introduced a *tert*-butyl substituent onto the carbamate group. This substitution was tolerated for NAAA inhibition but caused a lack of stereoselectivity, with IC_{50} values of 0.58 and 0.50 μM for (*S*) (**17a**) and (*R*) (**17b**) enantiomers, respectively. The second modification was the introduction of a methyl group at the β -position of the ring. Within the class of *N*-(2-oxo-3-oxetanyl)amides, *syn* methyl derivatives showed reduced inhibitory potency (IC_{50} values of $>100 \mu M$ for **8** and 100 μM for its enantiomer),³³ whereas the corresponding *anti* methyl derivatives were too unstable to be prepared or isolated (unpublished results); however, methyl substitution could be positively related to stability [e.g., compound **8** (Table 1 and related results)]. The first of the two benzyl derivatives **23a** and **23b**, formally related to *L*- and *D*-threonine, respectively, was slightly (10 times) more potent than the second. In the case of the *tert*-butyl carbamates (**24a–d**), it was possible to synthesize and test the four enantiomers corresponding to the relative configurations of the two substituents on the β -lactone ring. Among them, those having the C_β of the α -amino- β -lactone ring in the (*S*) configuration (**24b** and **24c**) were endowed with good inhibitory potency (IC_{50} values of 0.22 and 0.19 μM , respectively), while their enantiomers were inactive (for **24a**, $IC_{50} > 80 \mu M$) or significantly less potent (for **24d**, $IC_{50} = 4.9 \mu M$). The role of the lipophilicity of the carbamic acid ester side chain was explored with the introduction of a 5-phenylpentyl substituent (**27**). This compound showed a very good potency with respect to rat NAAA inhibition, with an IC_{50} of 127 nM, which demonstrates the positive influence of lipophilicity on rat NAAA inhibition.

Chemical Stability of *N*-(2-Oxo-3-oxetanyl)carbamic Acid Esters. The decision to move from serine- to threonine-based carbamic acid esters was conducive to chemical stability. For example, half-lives of threonine lactone **23b** were on

Table 2. Inhibitory Potencies (IC_{50}) of Compounds 10a,b, 11a,b, 13, 15, 17a,b, 19a,b, 23a,b, 24a–d, and 27 on Rat NAAA Activity

Cpds.	Structure	IC_{50} (μ M) \pm S.E.M.
10a		2.96 \pm 0.30
10b		0.70 \pm 0.10
11a		> 100
11b		> 100
13		> 100
15		> 100
17a		0.58 \pm 0.20
17b		0.50 \pm 0.14
19a		15.0 \pm 4.7
19b		49.2 \pm 15.0
23a		10.0 \pm 4.0
23b		1.0 \pm 0.2
24a		> 80
24b		0.22 \pm 0.03
24c		0.19 \pm 0.04
24d		4.9 \pm 0.7
27		0.13 \pm 0.03

average >4-fold longer than that of its homologue serine-based 10a (Table 3). A similar lengthening of half-lives was also

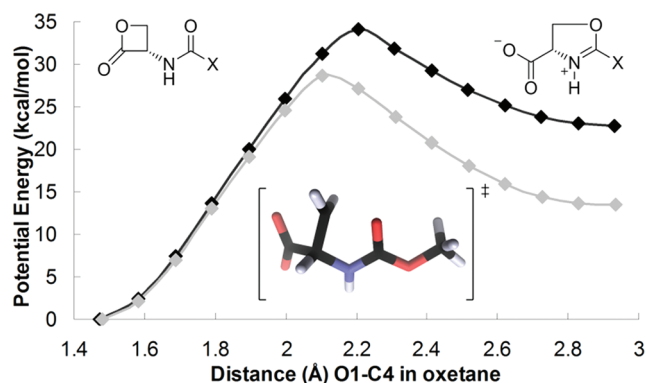


Figure 4. DTF potential energy surfaces for the nucleophilic attack of the side chain carbonyl oxygen at C_{β} of the β -lactone ring for two model compounds. Energies were calculated in the gas phase at the B3LYP/6-31+G(d) level of theory. The black curve is calculated for a carbamate derivative ($X = OCH_3$), and the gray curve refers to the same process for an amide derivative ($X = CH_3$). The increasing distances between the oxygen and C_{β} atoms in the oxetane ring are reported on the abscissa as the reaction coordinate. The inset structure represents the transition state structure, as calculated for the carbamate derivative.

Table 3. In Vitro Chemical Stabilities of Compounds 10a, 17a, 19a, 23b, 24a–c, and 27

compd	$t_{1/2}$ (min)		
	pH 7.4	pH 5.0	pH 5.0 with DTT
10a	26.7 \pm 2.0	39.2 \pm 1.8	30.5 \pm 2.9
17a	33.7 \pm 3.6	43.4 \pm 3.9	39.0 \pm 1.4
19a	3.3 \pm 1.2	29.7 \pm 2.7	25.1 \pm 4.0
23b	107.7 \pm 2.2	185.1 \pm 0.7	127.2 \pm 1.6
24a	143.4 \pm 1.1	217.0 \pm 9.4	149.2 \pm 3.4
24b	121.6 \pm 1.5	241.2 \pm 1.4	146.7 \pm 4.7
24c	80.7 \pm 1.6	93.8 \pm 0.8	80.4 \pm 0.2
27	110.3 \pm 3.4	194.2 \pm 3.0	134.4 \pm 1.5

observed for all other threonine-based derivatives 24a–c and 27. The introduction of a bulky *tert*-butyl substituent onto the carbamate side chain had no additive effect on chemical stability; within this subset of derivatives, *syn* 24b was more stable than the *anti* derivative (24c). Other threonine lactones, characterized by the *syn* arrangement, showed half-lives of >100 min at pH 7.4 and 5.0.

Biological Stability. The *N*-(2-oxo-3-oxetanyl)amides and *N*-(2-oxo-3-oxetanyl)carbamic acid esters were also assayed for their biological stability in the presence of a prototypical off-target protein, bovine serum albumin (BSA), the most abundant protein in plasma, which is also endowed with esterase activity,^{54,55} and 80% (v/v) rat plasma; this is a well-established in vitro model for hydrolytic metabolism.⁵⁶ Results are reported in Table 4.

In the presence of 20 mg/mL BSA, half-lives of all compounds significantly decreased with respect to chemical stability assays. Threonine-based derivatives were in general more stable than their serine-based analogues, which confirmed the important role of methyl substitution of the β -lactone system in chemical and BSA-catalyzed hydrolysis. For example, 1 had a half-life of 7.0 min in the presence of BSA, which doubled for threonine-based amide 8 ($t_{1/2} = 16$ min). In the set of carbamic acid esters, the very low stability of 10a ($t_{1/2} \sim 1$ min) was improved in analogues 23b ($t_{1/2} \sim 5$ min) and 27

Table 4. In Vitro Biological Stabilities for Compounds 1–9, 10a, 17a, 19a, 23b, 24a–c, and 27

compd	20 mg/mL BSA $t_{1/2}$ (min)	80% (v/v) rat plasma $t_{1/2}$ (s)
1	7.0 ± 0.6	<10
2	<1	<10
3	3.2 ± 0.7	75 ± 20
4	<1	29 ± 8
5	2.7 ± 0.6	<10
6	5.8 ± 1.0	65 ± 30
7	3.3 ± 0.8	32 ± 15
8	16.0 ± 1.2	<10
9	15.1 ± 1.8	14 ± 9
10a	1.2 ± 0.7	<10
17a	19.6 ± 1.5	<10
19a	4.6 ± 1.1	<10
23b	5.1 ± 0.8	<10
24a	120.7 ± 1.1	13 ± 6
24b	129.1 ± 7.0	11 ± 5
24c	87.7 ± 2.3	<10
27	11.4 ± 2.4	<10

($t_{1/2} \sim 11$ min). Nevertheless, the most relevant stabilization over BSA-catalyzed cleavage was obtained by the introduction of the bulky *tert*-butyl substituent on the carbamic acid ester side chain. The substitution of the benzyl (as in 10a) with a *tert*-butyl group (as in 17a) had a marked effect on stability, with the half-life increasing from ~ 1 to ~ 20 min. The effect was more pronounced in the case of threonine-based *tert*-butyl carbamic acid esters 24a–c. In fact, they showed half-lives, in the presence of BSA, comparable to those observed in pH 7.4 buffered solution, indicating no significant BSA-catalyzed cleavage and chemical stability as the limiting factor for these compounds. With compound 24b, for example, it was possible to maintain a good inhibitory potency on rat NAAA ($IC_{50} = 0.22 \mu M$) and half-lives of ~ 2 h in the case of both chemical and BSA-catalyzed hydrolysis.

The majority of the compounds were rapidly cleaved in the presence of 80% (v/v) rat plasma, with half-lives shorter than 1–2 min. To obtain preliminary indications of which types of plasma hydrolases might be responsible for the rapid degradation of the molecules, 24b was chosen as a representative of its class and subjected to a panel of stability assays in rat and human plasma in the presence of different enzymatic inhibitors.

Rat and human plasma contain different types of esterases,⁵⁷ including carboxylesterases, cholinesterases, and paraoxonase. Paraoxonase^{58–60} is a lipoprotein-associated esterase that hydrolyzes organophosphorous compounds but is not inhibited by them and is responsible for the cleavage of several arylesters and aromatic and aliphatic lactones; it requires calcium ions as a cofactor for activity and stability and is consequently inactivated by ethylenediaminetetraacetic acid (EDTA).^{61,62} The esterase inhibitors bis-4-nitrophenylphosphate (BNPP),⁶³ phenylmethanesulfonyl fluoride (PMSF),⁶⁴ and eserine were employed for the inhibition of carboxylesterases and cholinesterases, while EDTA was employed for the inhibition of calcium-dependent paraoxonase.⁶²

Table 5 reports the stability of compound 24b in rat and human plasma with different esterase inhibitors. In rat plasma, the cleavage of the compound was more rapid than in human plasma. This could depend on the higher esterase activity of the latter, as well as differences in enzyme composition.⁶⁵ In rat

Table 5. Plasma Stability of Compound 24b in the Presence of Enzymatic Inhibitors

inhibitor	$t_{1/2}$ (min)	
	50% (v/v) rat plasma	50% (v/v) human plasma
none	0.53 ± 0.20	2.99 ± 0.54
EDTA	0.34 ± 0.18	31.99 ± 2.60
BNPP	3.29 ± 1.70	4.70 ± 1.80
eserine	4.19 ± 0.90	13.75 ± 3.00
PMSF	7.13 ± 1.70	11.50 ± 2.80

plasma, the cleavage of 24b seems to be mainly dependent on the combined action of carboxylesterase and cholinesterase. In fact, while EDTA did not change the stability of the compound ($t_{1/2} = 0.53$ min vs 0.34 min in the presence of EDTA), BNPP, PMSF, and eserine markedly increased the half-life of 24b. In human plasma, which does not contain carboxylesterases,⁶⁵ inhibition of calcium-dependent esterases by EDTA led to a 10-fold increase in the half-life, a value higher than that observed with other inhibitors. Human plasma paraoxonase had already been identified as the main factor responsible for the quick plasma hydrolysis of a set of anti-inflammatory glucocorticoid γ -lactones.⁶⁶ In that case, a potential application of these compounds as “soft drugs” for the treatment of asthma was postulated,⁶⁷ based on the nonubiquitous distribution of paraoxonase, and in particular on its absence from the lung tissue.⁶¹ Soft drugs exert their therapeutic action in the target tissue and are then converted into inactive metabolites upon reaching the systemic circulation. In the literature, the soft drug strategy has been successfully exploited for topically applied drugs. With regard to the field of anti-inflammatory corticosteroids, attention was paid to carboxylic (thio)ester derivatives and the development of related plasma labile soft drugs^{67,68} or “antedrugs”.^{69,70} In the dermatologic field, boron-containing type 4 phosphodiesterase inhibitors, developed for topical treatment of psoriasis and atopic dermatitis, have been successfully derivatized by incorporation of a cleavable ester group, thus weakening their systemic side effects.⁷¹ With regard to our set of *N*-(2-oxo-3-oxetanyl)carbamic acid esters, low plasma stability may be turned to an advantage for topical applications. PEA is an endogenous component of the human epidermis and is generated from phospholipids in the stratum granulosum. Topical application of a PEA-containing product had been shown to significantly inhibit the development of UV light-induced erythema and thymine dimer formation in normal human skin.⁷² Topical application of plasma unstable NAAA inhibitors could therefore improve the anti-inflammatory effects of PEA, whereas the systemic instability of the compounds would restrict NAAA inhibition to the site of administration, thus weakening their potential systemic side effects.

CONCLUSIONS

A series of *N*-(2-oxo-3-oxetanyl)carbamic acid esters has been synthesized as rat NAAA inhibitors, and SARs and SPRs were studied to discover novel inhibitors endowed with an improved potency and stability profile. Figure 5 summarizes the SARs for the β -lactone carbamate NAAA inhibitors described here. They confirmed the importance of the β -lactone ring for rat NAAA inhibition and the positive role of the carbamate group in the side chain. The lipophilicity of the side chain was also positively correlated with NAAA inhibitory potency. The shift from serine- to threonine-based carbamic acid esters was tolerated in terms of NAAA inhibitory potency and led to an important

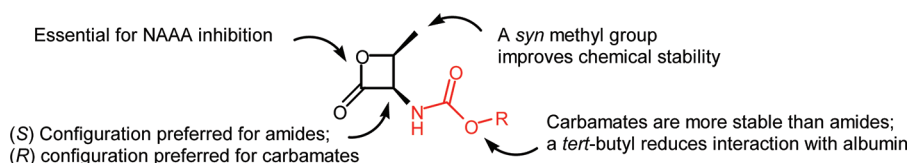


Figure 5. Summary of SARs for β -lactone carbamate inhibitors of NAAA.

improvement in the chemical stability profile, even if the preferred stereochemical configuration of the two substituents showed a complex and not yet fully defined dependence on the alkyl substitution of the carbamate side chain. The introduction of a bulky *tert*-butyl substituent into the side chain made the compounds less reactive toward BSA.

In particular, structural modulation led us to discover (2*S*,3*R*)-2-methyl-4-oxo-3-oxetanylcarbamic acid 5-phenylpentyl ester (**27**), which (i) is a potent *in vitro* rat NAAA inhibitor ($IC_{50} = 127$ nM), (ii) has an improved chemical stability profile, (iii) has a reduced propensity to react with BSA, and (iv) is rapidly cleaved by plasma hydrolases. Compound **27**, also termed URB913 and ARN077, is the first potent representative of a new class of NAAA inhibitors sharing a carbamic acid ester side chain, which has been expanded for further SAR investigation and potency improvement and reported elsewhere.⁷³ **27** may be a useful new tool for investigating the role of NAAA in inflammation and analgesia and a possible soft drug candidate for topical use.

EXPERIMENTAL SECTION

Chemicals, Materials, and Methods. All reagents were purchased from Sigma-Aldrich, Lancaster, Novabiochem, or Acros at the highest quality commercially available. Solvents were RP grade unless otherwise indicated. Dry tetrahydrofuran was distilled over sodium and benzophenone. Dry dimethylformamide, dichloromethane, and triethylamine were used as supplied. Petroleum ether refers to alkanes with boiling points of 40–60 °C. Melting points were determined on a Büchi B-540 capillary melting point apparatus. The structures of the unknown compounds were unambiguously assessed by MS, ¹H NMR, ¹³C NMR, and IR. MS (EI) spectra were recorded with a Fisons Trio 1000 (70 eV) spectrometer; only molecular ions (M^+) and base peaks are given. ESI-MS spectra were recorded with a Waters Micromass ZQ spectrometer in a positive mode using a nebulizing nitrogen gas at 400 L/min and a temperature of 250 °C, a cone flow of 40 mL/min, a capillary of 3.5 kV, and a cone voltage of 60 V; only molecular ions in positive or negative ion mode ($[M + H]^+$ or $[M - H]^-$, respectively) are given. ¹H NMR and ¹³C NMR spectra were recorded on Bruker AC 200 and 50 spectrometers, respectively, and analyzed using WIN-NMR. Chemical shifts were measured by using the central peak of the solvent. IR spectra were recorded on a Nicolet Atavar 360 FT spectrometer. Optical rotations were measured on a Perkin-Elmer 241 digital polarimeter using a sodium lamp (589 nm) as the light source; concentrations are expressed as grams per 100 mL, and the cell length was 1 dm. Enantiomeric excess (ee) values were determined by direct HPLC analysis with a Shimadzu spectrometer: pump LC-10AS, UV detector SPD-10A, integrator C-R6A, and the chiral column Chiralpak AD-H (0.46 cm \times 25 cm) using a combination of *n*-hexane and 2-propanol as the eluent. Column chromatography purifications were performed under “flash” conditions using Merck 230–400 mesh silica gel. TLC was conducted on Merck silica gel 60 F254 plates, which were visualized by being exposed to ultraviolet light and to an aqueous solution of ceric ammonium molybdate. Reactions involving generation or consumption of β -lactone were conveniently followed by TLC, using bromocresol green spray (0.04% in EtOH, made blue by addition of NaOH) followed by heating of the plate to detect the β -lactone as a yellow spot against a blue background. The final compounds were analyzed on a Thermo-

Quest (Italy) FlashEA 1112 elemental analyzer for C, H, and N. Analyses were within $\pm 0.4\%$ of the theoretical values. All tested compounds were $>95\%$ pure as determined by elemental analysis.

Rat plasma was obtained from male Wistar rats (250–300 g) (Charles River Laboratories, Milan, Italy). Animals were housed, handled, and cared for according to European Community Council Directive 86 (609) EEC, and the experimental protocol was conducted in compliance with Italian regulations (DL 116/92) and with local ethical committee guidelines for animal research. Pooled plasma was obtained by cardiac puncture, collected into heparinized tubes, centrifuged (1900g and 4 °C for 10 min) using an ALC refrigerated centrifuge (ALC srl, Cologno Monzese, Italy), and stored at -70 °C until it was used. BNPP, BSA, EDTA, eserine salicylate, human plasma, and PMSF were obtained from Sigma (Sigma-Aldrich srl, Milan, Italy).

Synthesis of (R)-2-Oxo-3-oxetanylcarbamic Acid Benzyl Ester (10b).³⁷ The compound was prepared by means of a two-step procedure reported in the literature:³⁶ white solid; mp 133–134 °C ($CHCl_3/n$ -hexane) [lit.³⁶ 133–134 °C ($CHCl_3/n$ -hexane)]; $[\alpha]_D^{20} = +31$ (c 0.5, CH_3CN) [lit.³⁶ $[\alpha]_D^{26} = +34.2$ (c 0.5, CH_3CN)]; ee $>98\%$ (Chiral HPLC, AD-H; flow, 1 mL/min; λ_{max} 220 nm; eluent, 9:1 *n*-hexane/*i*-PrOH; $t_R = 17.9$ min); MS (EI) m/z 221 (M^+), 91 (100); ¹H NMR ($CDCl_3$) δ 4.45–4.48 (m, 2H), 5.15 (m, 3H), 5.51 (br s, 1H), 7.37 (m, 5H); ¹³C NMR ($CDCl_3$) δ 59.6, 65.3, 67.8, 128.4, 128.6, 128.7, 135.4, 155.2, 168.7; IR (Nujol) ν_{max} 3365, 1847, 1831, 1684, 1532 cm^{-1} . Anal. ($C_{11}H_{11}NO_4$) C, H, N.

Synthesis of Cyclobutylcarbamic Acid Benzyl Ester (13).³⁸ To a stirred solution of $NaHCO_3$ (0.504 g, 6.0 mmol) in H_2O (7.0 mL) were added *c*- $C_4H_7NH_2$ (0.213 g, 0.260 mL, 3.0 mmol) and, dropwise, **12** (0.512 g, 0.430 mL, 3.0 mmol). The mixture was stirred at room temperature for 3 h, diluted with H_2O (10 mL), and extracted with EtOAc. The combined organic phases were washed with brine, dried (Na_2SO_4), and concentrated. Purification of the residue by flash column chromatography (8:2 cyclohexane/EtOAc) and recrystallization gave **13** as white needles: 67% yield (0.410 g); mp 75–76 °C (Et_2O /petroleum ether); MS (EI) m/z 205 (M^+), 91 (100); ¹H NMR ($CDCl_3$) δ 1.61–1.96 (m, 4H), 2.26–2.41 (m, 2H), 4.08–4.24 (m, 1H), 4.89 (br s, 1H), 5.09 (s, 2H), 7.36 (m, 5H); ¹³C NMR ($CDCl_3$) δ 14.7, 31.4, 46.2, 66.5, 128.1, 128.5, 136.6, 155.2; IR (neat) ν_{max} 3317, 2977, 2945, 1682, 1539 cm^{-1} . Anal. ($C_{12}H_{13}NO_2$) C, H, N.

Synthesis of (R,S)-2-Oxocyclobutylcarbamic Acid Benzyl Ester (15).³⁶ The compound was prepared following a literature procedure:³⁶ colorless oil; MS (EI) m/z 220 ($[M + 1]^+$), 91 (100); ¹H NMR ($CDCl_3$) δ 1.94–2.14 (m, 1H), 2.38–2.56 (m, 1H), 2.87–2.96 (m, 2H), 4.82–4.95 (m, 1H), 5.11 (s, 2H), 5.28 (br s, 1H), 7.36 (m, 5H); ¹³C NMR ($CDCl_3$) δ 19.8, 41.6, 65.2, 67.1, 128.2, 128.3, 128.6, 136.0, 155.4, 205.3; IR (neat) ν_{max} 3356, 3033, 2961, 1792, 1701, 1522 cm^{-1} . Anal. ($C_{12}H_{13}NO_3$) C, H, N.

(S)-(2-Oxo-3-oxetanyl)carbamic Acid *tert*-Butyl Ester (17a).³⁷ For the white solid, the yield, mp, $[\alpha]_D^{20}$, and MS (EI) are given in ref 33. ¹H NMR and IR data are given in ref 37. Anal. ($C_8H_{13}NO_4$) C, H, N.

(R)-(2-Oxo-3-oxetanyl)carbamic Acid *tert*-Butyl Ester (17b).⁴² For the white solid, the yield, mp, $[\alpha]_D^{20}$, MS (EI), ¹H NMR, and IR are given in ref 33. Anal. ($C_8H_{13}NO_4$) C, H, N.

Synthesis of (S)-1-Methyl-3-(2-oxo-3-oxetanyl)urea (19a). To a stirred mixture of **18a** (0.130 g, 0.5 mmol) in dry THF (4 mL), at 0 °C under a N_2 atmosphere, were added Et_3N (0.056 g, 0.085 mL, 0.55 mmol) and $C_6H_5CH_2NCO$ (0.073 g, 0.068 mL, 0.55 mmol). The mixture was stirred at 0 °C for 0.5 h and at room temperature for 3 h and then concentrated. Purification of the residue by column chromatography (4:6 to 2:8 cyclohexane/EtOAc) and recrystallization gave **19a** as white crystals: 54% yield (0.060 g); mp 188–190 °C,

decomposition with color change starting from 130 °C, sealed capillary tube [(CH₃)CO(CH₃)/petroleum ether]; [α]_D²⁰ = -12 (c 0.5, MeOH); MS (EI) *m/z* 220 (M⁺), 91 (100); ¹H NMR (DMSO-*d*₆) δ 4.20 (d, 2H, *J* = 6 Hz), 4.31–4.36 (m, 2H), 5.07–5.16 (m, 1H), 6.80–6.92 (m, 2H), 7.21–7.32 (m, 5H); ¹³C NMR (DMSO-*d*₆) δ 43.3, 59.2, 66.6, 127.1, 127.5, 128.7, 140.8, 157.4, 172.1; IR (Nujol) ν_{\max} 3421, 3295, 1845, 1651, 1545 cm⁻¹. Anal. (C₁₁H₁₂N₂O₃) C, H, N.

Synthesis of (R)-1-Methyl-3-(2-oxo-3-oxetanyl)urea (19b). The same protocol applied to **18b**, apart from the eluent for column chromatography (3:7 cyclohexane/EtOAc), gave **19b** as white crystals: 42% yield (0.060 g); mp 183 °C, decomposition with color change starting from 125 °C, sealed capillary tube [(CH₃)CO(CH₃)/petroleum ether]; [α]_D²⁰ +10 (c 0.5, MeOH); MS (EI) *m/z* 220 (M⁺), 91 (100); ¹H NMR (DMSO-*d*₆) δ 4.21 (d, 2H, *J* = 6 Hz), 4.29–4.37 (m, 2H), 5.08–5.17 (m, 1H), 6.78–6.87 (m, 2H), 7.17–7.32 (m, 5H); ¹³C NMR (DMSO-*d*₆) δ 43.3, 59.2, 66.6, 127.1, 127.5, 128.7, 140.8, 157.4, 172.1; IR (Nujol) ν_{\max} 3421, 3295, 1845, 1651, 1545 cm⁻¹. Anal. (C₁₁H₁₂N₂O₃) C, H, N.

General Procedure for the Synthesis of Threonine β -Lactones 23a,b and 24a–d. To a stirred mixture of the opportune *N*-Cbz- and *N*-Boc-threonine (**21a,b** and **22a–d**) (3.65 mmol) in dry CH₂Cl₂ (75 mL), at 0 °C and under a N₂ atmosphere, were added Et₃N (1.1 g, 1.53 mL, 10.95 mmol) and BOP reagent (1.946 g, 4.4 mmol). The mixture was stirred at 0 °C for 1 h and at room temperature for 2 h (**23a,b**) or at room temperature for 3 h (**24a–d**) and then concentrated. Purification of the residue by column chromatography (8:2 cyclohexane/EtOAc for **23a**, 7:3 cyclohexane/EtOAc for **23b** and **24c,d**, and 1:1 cyclohexane/EtOAc for **24a,b**) and recrystallization gave **23a,b** and **24a–d**.

(2R,3S)-2-Methyl-4-oxo-3-oxetanylcarbamic Acid Benzyl Ester (23a):⁴³ white needles; 50% yield (0.429 g); mp 120–122 °C (CHCl₃/*n*-hexane); [α]_D²⁰ +11.0 [c 0.29, (CH₃)CO(CH₃)]; MS (EI) *m/z* 235 (M⁺), 91 (100); ¹H NMR (DMSO-*d*₆) δ 1.33 (d, 3H, *J* = 6.3 Hz), 4.85 (m, 1H), 5.01–5.14 (ABq, 2H), 5.44 (dd, 1H, *J*₁ = 9.4 Hz, *J*₂ = 6.1 Hz), 7.27–7.43 (m, 5H), 8.36 (d, 1H, *J* = 9.4 Hz); ¹³C NMR (CDCl₃) δ 15.1, 60.4, 67.9, 74.7, 128.3, 128.6, 128.7, 135.5, 155.3, 168.7; IR (Nujol) ν_{\max} 3284, 1813, 1695, 1553 cm⁻¹. Anal. (C₁₂H₁₃NO₄) C, H, N.

(2S,3R)-2-Methyl-4-oxo-3-oxetanylcarbamic Acid Benzyl Ester (23b): white solid; 55% yield (0.472 g); mp 120–121 °C (CHCl₃/*n*-hexane); [α]_D²⁰ -9.5 [c 0.2, (CH₃)CO(CH₃)]; MS (EI) *m/z* 235 (M⁺), 91 (100); ¹H NMR (DMSO-*d*₆) δ 1.33 (d, 3H, *J* = 6.4 Hz), 4.85 (m, 1H), 5.01–5.14 (ABq, 2H), 5.44 (dd, 1H, *J* = 9.4, 6.1 Hz), 7.27–7.43 (m, 5H), 8.36 (d, 1H, *J* = 9.4 Hz); ¹³C NMR (CDCl₃) δ 15.1, 60.4, 67.9, 74.7, 128.3, 128.6, 128.7, 135.5, 155.3, 168.7; IR (Nujol) ν_{\max} 3284, 1813, 1695, 1553 cm⁻¹. Anal. (C₁₂H₁₃NO₄) C, H, N.

(2R,3S)-2-Methyl-4-oxo-3-oxetanylcarbamic Acid tert-Butyl Ester (24a):⁴⁴ For the off-white solid, the yield, mp, [α]_D²⁰, MS (EI), ¹H NMR, and IR are given in ref 33; ¹³C NMR (CDCl₃) δ 15.1, 28.2, 60.1, 74.9, 81.3, 154.4, 169.2. Anal. (C₉H₁₅NO₄) C, H, N. Anal. (C₉H₁₅NO₄) C, H, N.

(2S,3R)-2-Methyl-4-oxo-3-oxetanylcarbamic Acid tert-Butyl Ester (24b):³³ For the white solid, the yield, mp, [α]_D²⁰, MS (EI), ¹H NMR, and IR are given in ref 33; ¹³C NMR (CDCl₃) δ 15.1, 28.2, 60.1, 74.9, 81.3, 154.4, 169.2. Anal. (C₉H₁₅NO₄) C, H, N.

(2S,3S)-allo-2-Methyl-4-oxo-3-oxetanylcarbamic Acid tert-Butyl Ester (24c): white crystal; 76% yield (0.566 g); mp 119–121 °C (CHCl₃/*n*-hexane); [α]_D²⁰ -81.7 (c 0.45, MeOH); MS (EI) *m/z* 202 (M⁺), 146 (100); ¹H NMR (CDCl₃) δ 1.47 (s, 9H), 1.61 (d, 3H, *J* = 6.1 Hz), 4.59 (m, 1H), 4.69–4.80 (m, 1H), 5.14 (br s, 1H); ¹³C NMR (CDCl₃) δ 18.9, 28.2, 64.3, 76.9, 81.4, 154.4, 168.1; IR (Nujol) ν_{\max} 3357, 1828, 1689, 1534 cm⁻¹. Anal. (C₉H₁₅NO₄) C, H, N.

(2R,3R)-allo-2-Methyl-4-oxo-3-oxetanylcarbamic Acid tert-Butyl Ester (24d): white crystal; 75% yield (0.558 g); mp 119–121 °C (CHCl₃/*n*-hexane); [α]_D²⁰ +81.8 (c 0.4, MeOH); MS (EI) *m/z* 202 (M⁺), 146 (100); ¹H NMR (CDCl₃) δ 1.47 (s, 9H), 1.61 (d, 3H, *J* = 6.2 Hz), 4.58–4.61 (m, 1H), 4.69–4.80 (m, 1H), 5.14 (br s, 1H); IR (Nujol) ν_{\max} 3356, 1828, 1690, 1540 cm⁻¹; ¹³C NMR (CDCl₃) δ 18.9, 28.2, 64.3, 76.9, 81.4, 154.4, 168.1. Anal. (C₉H₁₅NO₄) C, H, N.

Synthesis of (2S,3R)-2-Methyl-4-oxo-3-oxetanylcarbamic Acid 5-Phenylpentyl Ester (27). To a stirred solution of **26** (0.430 g, 1.4

mmol) and Et₃N (0.425 g, 0.585 mL, 4.2 mmol) in dry CH₂Cl₂ (20 mL), at 0 °C and under a N₂ atmosphere, was added HBTU (0.796 g, 2.1 mmol). The mixture was stirred at 0 °C for 3 h and at room temperature for 6 h and then concentrated. Purification of the residue by flash column chromatography (7:3 cyclohexane/EtOAc) and trituration gave **27** as an off-white solid: 7% yield (0.030 g); mp 80–83 °C (*n*-hexane); [α]_D²⁰ = -68.2 [c 0.11, (CH₃)CO(CH₃)]; MS (EI) *m/z* 292 [(M + 1)⁺], 91 (100); ¹H NMR [(CD₃)CO(CD₃)] δ 1.34–1.47 (m, 5H), 1.57–1.69 (m, 4H), 2.62 (t, 2H, *J* = 7.5 Hz), 4.00–4.10 (m, 2H), 4.85–4.97 (m, 1H), 5.49–5.56 (dd, 1H, *J*₁ = 4.6 Hz, *J*₂ = 6.3 Hz), 7.16–7.28 (m, 6H); ¹³C NMR [(CD₃)CO(CD₃)] δ 14.2, 25.3, 28.7, 31.1, 35.5, 60.4, 65.0, 74.4, 125.6, 128.2, 128.3, 142.4, 155.8, 169.2; IR (Nujol) ν_{\max} 3452, 3330, 1846, 1825, 1694, 1655, 1541 cm⁻¹. Anal. (C₁₆H₂₁NO₄) C, H, N.

(S)-2-Oxo-3-oxetanyl ammonium Toluene-4-sulfonate (18a):⁴⁰ For the white solid, the yield, mp, and ¹H NMR are given in ref 40.

(R)-2-Oxo-3-oxetanyl ammonium Toluene-4-sulfonate (18b):⁴¹ For the white solid, the ¹H NMR is given in ref 41.

General Procedure for the Synthesis of Threonine Derivatives 21a,b and 22a–d. To a stirred mixture of the opportune threonine **20a–d** (1 g, 8.4 mmol) and NaHCO₃ (1.76 g, 21 mmol, **21a,b**; 1.092 g, 13 mmol, **22a–d**) in H₂O (17 mL) and THF (8.5 mL) (in the case of **21a,b**) or MeOH (17 mL) (in the case of **22a–d**) was added **12** dropwise over 0.5 h (1.58 g, 1.32 mL, 9.24 mmol) (**21a,b**) or Boc₂O (2.684 g, 12.3 mmol) (**22a–d**). The mixture was stirred at room temperature (1 h for **21a,b**; 14 h for **22a–d**), concentrated, supplemented with Et₂O, acidified with 2 N HCl, and extracted with EtOAc. The combined organic layers were washed with brine, dried (Na₂SO₄), and concentrated to give **21a,b** and **22a–d**.

(2S,3R)-2-Benzoyloxycarbonylamino-3-hydroxybutyric Acid (21a):⁴⁵ 54% yield (1.13 g); [α]_D²⁰ -2.2 (c 1.6, MeOH); HPLC/ESI(+) *m/z* 254 (M⁺), 271 (M + NH₄); ¹H NMR (CDCl₃) δ 1.09–1.27 (m, 3H), 4.32–4.41 (m, 2H), 5.03–5.16 (m, 2H), 6.03 (br d, 1H), 6.25 (br s, 2H), 7.32 (m, 5H); IR (neat) ν_{\max} 3338, 2974, 1716, 1531 cm⁻¹.

(2R,3S)-2-Benzoyloxycarbonylamino-3-hydroxybutyric Acid (21b):⁴⁶ 76% yield (1.67 g); [α]_D²⁰ +2.5 (c 1.9, MeOH); HPLC/ESI(+) *m/z* 254 (M⁺), 271 (M + NH₄); ¹H NMR (CDCl₃) δ 1.09–1.27 (m, 3H), 4.32–4.41 (m, 2H), 5.03–5.16 (m, 2H), 6.03 (br d, 1H), 6.25 (br s, 2H), 7.32 (m, 5H); IR (neat) ν_{\max} 3338, 2974, 1716, 1531 cm⁻¹.

(2S,3R)-2-tert-Butoxycarbonylamino-3-hydroxybutyric Acid (22a):⁴⁷ The yield, MS (EI), and ¹H NMR are given in ref 33.

(2R,3S)-2-tert-Butoxycarbonylamino-3-hydroxybutyric Acid (22b):⁴⁸ The yield, MS (EI), and ¹H NMR are given in ref 33.

(2R,3R)-allo-2-tert-Butoxycarbonylamino-3-hydroxybutyric Acid (22c):⁴⁹ 78% yield (1.44 g); ¹H NMR (CDCl₃) δ 1.29 (m, 3H), 1.47 (s, 9H), 4.08–4.38 (m, 2H), 5.54 (br d, 1H), 5.84 (br s, 2H).

(2S,3S)-allo-2-tert-Butoxycarbonylamino-3-hydroxybutyric Acid (22d):⁵⁰ 95% yield (1.75 g); ¹H NMR (CDCl₃) δ 1.28 (d, 3H), 1.46 (s, 9H), 4.08–4.38 (m, 2H), 5.60 (br s, 1H), 6.55 (br d, 2H).

Synthesis of (2R,3S)-3-Hydroxy-2-(5-phenylpentyl)oxycarbonylamino)butyric Acid (26). To a stirred suspension of NaHCO₃ (0.622 g, 7.4 mmol) in THF (1.6 mL) and H₂O (3.3 mL) was carefully added **20b** (0.353 g, 2.96 mmol). After gas evolution, 5-phenylpentyl chloroformate (0.740 g, 3.26 mmol), previously prepared as reported in the literature,⁵² was added slowly followed by (*n*-Bu)₄NBr (0.035 g, 0.92 mmol). The mixture was stirred at room temperature for 18 h, diluted with H₂O, and washed with Et₂O. The aqueous phase was acidified to pH 2 with 2 N HCl and extracted with EtOAc. The combined organic phases were washed with brine, dried (Na₂SO₄), filtered, and concentrated to give **26** as a colorless oil: 48% yield (0.440 g); HPLC/ESI *m/z* 310 (M⁺), 308 (M⁺); ¹H NMR [(CD₃)CO(CD₃)] δ 1.14–1.24 (m, 5H), 1.36–1.48 (m, 2H), 1.58–1.72 (m, 4H), 2.62 (t, 2H, *J* = 7.6 Hz), 4.05 (q, 2H, *J* = 7.1 Hz), 4.14–4.50 (m, 2H), 5.92 (br d, 1H), 7.12–7.31 (m, 5H); ¹³C NMR [(CD₃)CO(CD₃)] δ 19.7, 25.3, 28.8, 31.1, 35.5, 59.2, 64.4, 67.0, 125.6, 128.2, 128.3, 142.5, 156.8, 171.6; IR (Nujol) ν_{\max} 3347, 1716, 1530 cm⁻¹.

In Vitro Chemical Stability. Chemical stability was investigated at a fixed ionic strength (μ = 0.15 M) under physiological [0.01 M

phosphate-buffered saline (PBS) (pH 7.4)] and acidic [0.01 M phosphate buffer (pH 5.0)] pH conditions, and in the presence of a 3 mM solution of the thiol nucleophile DTT in 0.01 M phosphate buffer (pH 5.0), as previously reported.⁷⁴ Stock solutions of compounds were prepared in DMSO, and each sample was incubated at a final concentration of 1–100 μM in a prewarmed (37 °C) buffer solution; the final DMSO concentration in the samples was kept at 1%. The samples were maintained at 37 °C in a temperature-controlled shaking water bath (60 rpm). At various time points, 100 μL aliquots were removed and analyzed by HPLC. Apparent half-lives ($t_{1/2}$) for the disappearance of test compounds were calculated from the pseudo-first-order rate constants obtained by linear regression of plots of $\log[\text{compound}]$ versus time and are listed in Tables 1 and 3 as mean values of three experiments along with their standard deviations.

In Vitro Rat Plasma Stability. Rat plasma stability was investigated as previously reported.⁷⁴ Briefly, plasma was quickly thawed and diluted to 80% (v/v) with PBS (pH 7.4) to buffer the solution pH, which was checked during the course of the experiments. Pooled rat plasma (400 μL) was incubated with PBS buffer (95 μL , pH 7.4) and a compound stock solution (5 μL) in DMSO (final DMSO concentration in samples of 1%; final compound concentrations of 5–100 μM). Samples were maintained at 37 °C in a temperature-controlled shaking water bath (60 rpm) throughout the experiments. At regular time points, aliquots (50 μL) were withdrawn, supplemented with 2 volumes of CH_3CN , centrifuged at 8000g for 5 min at 4 °C, and analyzed by RP-HPLC. Apparent half-lives ($t_{1/2}$) for the disappearance of test compounds were calculated from the pseudo-first-order rate constants obtained by linear regression of plots of $\log[\text{compound}]$ versus time; apparent half-life values listed in Table 4 as the mean values of three experiments along with standard deviations.

In Vitro Stability in the Presence of BSA. A 20 mg/mL solution of bovine serum albumin in PBS (pH 7.4) was employed for stability assays at 37 °C. Test compounds were incubated at final concentrations of 5–100 μM with a final DMSO percentage of 1% (v/v). Samples were processed as reported above for rat plasma stability experiments.

In Vitro Rat and Human Plasma Stability in the Presence of Selected Inhibitors. Rat and human plasma stability experiments in the presence of selected inhibitors (BNPP, eserine, PMSF, and EDTA) took place at 37 °C in the presence of 50% (v/v) plasma, because of the very rapid hydrolysis of the test compounds under the previously reported experimental conditions [80% (v/v) plasma at 37 °C]. Briefly, rat and human plasma were preincubated in the presence of selected inhibitors or vehicle according to literature conditions.⁶⁵ After preincubation, compound **24b** was added, and at regular time points, aliquots of the sample (50 μL) were withdrawn, processed, and analyzed as reported for in vitro rat plasma stability assays.

Conditions for HPLC–UV–MS Analysis. The degradation of compounds **1–9**, **10a**, **19a**, and **23b** was monitored by RP-HPLC and UV by employing a Shimadzu gradient system (Shimadzu Corp., Kyoto, Japan) consisting of two Shimadzu LC-10ADvp solvent delivery modules, a 20 μL Rheodyne sample injector (Rheodyne LLC, Rohnert Park, CA), and an SPD-10Avp UV–vis detector, equipped with a reversed-phase C_{18} column [LC-18-DB, 5 μm , 150 mm \times 4.6 mm (inside diameter) (Supelco, Bellefonte, PA)]. The HPLC system was interfaced with PeakSimple version 2.83 for data acquisition. Mobile phases consisted of various percentages of CH_3CN and 0.1% (v/v) formic acid delivered at a flow rate of 1 mL/min. Each compound was monitored at its relative absorbance maximum for UV detection. Compounds **17a**, **24a–c**, and **27** were monitored with an API150EX single-quadrupole HPLC–MS system (AB/Sciex, Toronto, ON) equipped with an atmospheric pressure chemical ionization (APCI) ion source working in positive and negative ion mode and coupled to an Agilent 1100 series HPLC system (Agilent Technologies, Waldbronn, Germany) that consisted of a G1312A binary pump, a G1379A degasser, and a 10 μL Rheodyne sample injector. Compound-dependent parameters were optimized by flow injection analysis (FIA) and ramping of the potentials. The final settings were as follows: declustering potential (DP), ± 3.0 V; focusing

potential (FP), ± 100 V; entrance potential (EP), ± 10 V. In all cases, higher voltages led to compound in-source fragmentation. The ion source temperature was set at 400 °C. A Supelcosil C18-DB column (150 mm \times 4.6 mm, 5 μm) (Supelco) was employed; the flow rate was kept at 1 mL/min. Mobile phases consisted of various percentages of acetonitrile and 10 mM ammonium acetate (pH 7.0). Data were acquired by employing Analyst version 1.4 (AB/Sciex).

Pharmacology. NAAA Assay. Recombinant NAAA, expressed as described previously,³³ was incubated at 37 °C for 30 min in 0.2 mL of sodium hydrogen phosphate buffer (50 mM, pH 5.0) containing 0.1% Triton X-100, 3 mM dithiothreitol (DTT), and 50 mM heptadecenoylethanolamide as the substrate. The reaction was terminated by the addition of 0.2 mL of cold methanol containing 1 nmol of heptadecanoic acid (NuCheck Prep, Elysian, MN). Samples were analyzed by liquid chromatography and mass spectrometry. Heptadecenoic acid and heptadecanoic acid were eluted on an XDB Eclipse C18 column isocratically at 2.2 mL/min for 1 min with a solvent mixture of 95% methanol and 5% water, both containing 0.25% acetic acid and 5 mM ammonium acetate. The column temperature was 50 °C. ESI was conducted in the negative mode. The capillary voltage was 4 kV and the fragmentor voltage 100 V. N_2 was used as the drying gas at a flow rate of 13 L/min and 350 °C. The nebulizer pressure was set at 60 psi. $[\text{M} - \text{H}]^- = 267$ in the selected ion monitoring mode. Calibration curves were generated using commercial heptadecenoic acid (NuCheck Prep).

Quantum Mechanical Simulations of Reaction Kinetics. Three-dimensional structures of the model compounds (*S*)-4,5-dihydro-2-methyl-4-oxazolecarboxylic acid and (*S*)-4,5-dihydro-2-methoxy-4-oxazolecarboxylic acid were built in their zwitterionic forms (dihydro-4-oxazoliumcarboxylates) using Maestro,⁷⁵ and their geometry was optimized in the gas phase by means of DFT⁷⁶ calculation as implemented in Jaguar.⁷⁷ The B3LYP hybrid functional⁷⁸ was applied in combination with the 6-31+G(d) basis set, which includes polarization and diffuse function for non-hydrogen atoms. Default convergence criteria were applied during all the calculations performed. Starting from the corresponding minimal-energy structures, we explored the potential energy surfaces for the internal nucleophilic substitution by gradually shortening (i.e., in 0.1 Å steps) the distance between one of the oxygens of the 4-carboxylate group and the methylene carbon at position 5 of the 4,5-dihydroazole scaffold. Then, at each step of the reaction coordinate, the geometry of the system was optimized and its energy calculated at the B3LYP/6-31+G(d) level of theory. The O–C distance was the only restraint applied during the simulations, while other degrees of freedom were allowed to change during the optimization step. The reaction coordinate here employed yielded the two β -lactone derivatives, namely, (*S*)-*N*-(2-oxo-3-oxetanyl)acetamide and (*S*)-(2-oxo-3-oxetanyl)carbamic acid methyl ester, respectively, as products of the simulated reaction. Approximate transition state (TS) structures (corresponding to the points with the highest energy along the path) were also identified. The geometry and the energetics of these TSs were characterized more precisely by performing a linear synchronous transit search in Jaguar. Finally, stationary points were analyzed by the vibrational frequency calculations. The vibrational motion associated with the negative frequency, characteristic of transition states, resulted in the motion going toward products, in two opposite directions.

■ AUTHOR INFORMATION

Corresponding Author

*Phone: +39-0521-905059. Fax: +39-0521-905006. E-mail: marco.mor@unipr.it.

Notes

The authors declare no competing financial interest.

■ ACKNOWLEDGMENTS

This work was supported by MIUR (Ministero dell'Istruzione, dell'Università e della Ricerca) and Universities of Parma and Urbino "Carlo Bo".

■ DEDICATION

This article is dedicated to the memory of Andrea Tontini, who sadly died after the manuscript had been submitted. Andrea, a valuable scientist and a great friend, joined the research group in Urbino in 1991 and was a pillar of our teamwork. His sudden death leaves a professional void in our research groups and tremendous grief in our hearts.

■ ABBREVIATIONS USED

AEA, *N*-arachidonylethanolamine; AS, amidase signature; BNPP, bis-4-nitrophenylphosphate; BOP, benzotriazol-1-yloxytris(dimethylamino)phosphonium hexafluorophosphate; DFT, density functional theory; FAE, fatty acid ethanolamide; HBTU, 2-(1*H*-benzotriazol-1-yl)-1,1,3,3-tetramethylammonium hexafluorophosphate; HPLC, high-performance liquid chromatography; NAAA, *N*-acylethanolamine acid amidase; Ntn, *N*-terminal nucleophile; PEA, palmitoylethanolamide; PMSF, phenylmethanesulfonyl fluoride; PBS, phosphate-buffered saline; QM/MM, quantum mechanics/molecular mechanics; RP, reverse phase; SPR, structure–property relationship.

■ REFERENCES

- (1) Petrosino, S.; Iuvone, T.; Di Marzo, V. *N*-Palmitoyl-ethanolamine: Biochemistry and new therapeutic opportunities. *Biochimie* **2010**, *92*, 724–727.
- (2) Muccioli, G. Endocannabinoid biosynthesis and inactivation, from simple to complex. *Drug Discovery Today* **2010**, *15*, 474–483.
- (3) Minkkilä, A.; Saario, S.; Nevalainen, T. Discovery and development of endocannabinoid-hydrolyzing enzyme inhibitors. *Curr. Top. Med. Chem.* **2010**, *10*, 828–858.
- (4) Mazzari, S.; Canella, R.; Petrelli, L.; Marcolongo, G.; Leon, A. *N*-(2-Hydroxyethyl)hexadecanamide is orally active in reducing edema formation and inflammatory hyperalgesia by down-modulating mast cell activation. *Eur. J. Pharmacol.* **1996**, *300*, 227–236.
- (5) Calignano, A.; La Rana, G.; Giuffrida, A.; Piomelli, D. Control of pain initiation by endogenous cannabinoids. *Nature* **1998**, *394*, 277–281.
- (6) Lo Verme, J.; Fu, J.; Astarita, G.; La Rana, G.; Russo, R.; Calignano, A.; Piomelli, D. The nuclear receptor peroxisome proliferator-activated receptor- α mediates the anti-inflammatory actions of palmitoylethanolamide. *Mol. Pharmacol.* **2005**, *67*, 15–19.
- (7) Zhu, C.; Solorzano, C.; Sahar, S.; Realini, N.; Fung, E.; Sassone-Corsi, P.; Piomelli, D. Proinflammatory stimuli control *N*-acylphosphatidylethanolamine-specific phospholipase D expression in macrophages. *Mol. Pharmacol.* **2011**, *79*, 786–792.
- (8) D'Agostino, G.; La Rana, G.; Russo, R.; Sasso, O.; Iacono, A.; Esposito, E.; Raso, G. M.; Cuzzocrea, S.; Lo Verme, J.; Piomelli, D.; Meli, R.; Calignano, A. Acute intracerebroventricular administration of palmitoylethanolamide, an endogenous peroxisome proliferator-activated receptor- α agonist, modulates carrageenan-induced paw edema in mice. *J. Pharmacol. Exp. Ther.* **2007**, *322*, 1137–1143.
- (9) Calignano, A.; La Rana, G.; Piomelli, D. Antinociceptive activity of the endogenous fatty acid amide, palmitoylethanolamide. *Eur. J. Pharmacol.* **2001**, *419*, 191–198.
- (10) LoVerme, J.; Russo, R.; La Rana, G.; Fu, J.; Farthing, J.; Mattace-Raso, G.; Meli, R.; Hohmann, A.; Calignano, A.; Piomelli, D. Rapid broad-spectrum analgesia through activation of peroxisome proliferator-activated receptor- α . *J. Pharmacol. Exp. Ther.* **2006**, *319*, 1051–1061.
- (11) Devane, W. A.; Hanuš, L.; Breuer, A.; Pertwee, R. G.; Stevenson, L. A.; Griffin, G.; Gibson, D.; Mandelbaum, A.; Etinger, A.;

Mechoulam, R. Isolation and structure of a brain constituent that binds to the cannabinoid receptor. *Science* **1992**, *258*, 1946–1949.

- (12) Rodríguez de Fonseca, F.; Navarro, M.; Gómez, R.; Escuredo, L.; Nava, F.; Fu, J.; Murillo-Rodríguez, E.; Giuffrida, A.; LoVerme, J.; Gaetani, S.; Kathuria, S.; Gall, C.; Piomelli, D. An anorexic lipid mediator regulated by feeding. *Nature* **2001**, *414*, 209–212.

- (13) Fu, J.; Gaetani, S.; Oveisi, F.; Lo Verme, J.; Serrano, A.; Rodríguez De Fonseca, F.; Rosengarth, A.; Luecke, H.; Di Giacomo, B.; Tarzia, G.; Piomelli, D. Oleyethanolamide regulates feeding and body weight through activation of the nuclear receptor PPAR- α . *Nature* **2003**, *425*, 90–93.

- (14) Ueda, N.; Tsuboi, K.; Uyama, T. *N*-Acylethanolamine metabolism with special reference to *N*-acylethanolamine-hydrolyzing acid amidase (NAAA). *Prog. Lipid Res.* **2010**, *49*, 299–315.

- (15) Okamoto, Y.; Morishita, J.; Tsuboi, K.; Tonai, T.; Ueda, N. Molecular characterization of a phospholipase D generating anandamide and its congeners. *J. Biol. Chem.* **2004**, *279*, 5298–5305.

- (16) Liu, J.; Wang, L.; Harvey-White, J.; Osei-Hyiaman, D.; Razdan, R.; Gong, Q.; Chan, A. C.; Zhou, Z.; Huang, B. X.; Kim, H.-Y.; Kunos, G. A biosynthetic pathway for anandamide. *Proc. Natl. Acad. Sci. U.S.A.* **2006**, *103*, 13345–13350.

- (17) Di Marzo, V.; Fontana, A.; Cadas, H.; Schinelli, S.; Cimino, G.; Schwartz, J. C.; Piomelli, D. Formation and inactivation of endogenous cannabinoid anandamide in central neurons. *Nature* **1994**, *372*, 686–691.

- (18) McKinney, M. K.; Cravatt, B. F. Structure and function of fatty acid amide hydrolase. *Annu. Rev. Biochem.* **2005**, *74*, 411–432.

- (19) Tsuboi, K.; Takezaki, N.; Ueda, N. The *N*-acylethanolamine-hydrolyzing acid amidase (NAAA). *Chem. Biodiversity* **2007**, *4*, 1914–1925.

- (20) Ueda, N.; Yamanaka, K.; Yamamoto, S. Purification and characterization of an acid amidase selective for *N*-palmitoylethanolamine, a putative endogenous anti-inflammatory substance. *J. Biol. Chem.* **2001**, *276*, 35552–35557.

- (21) Tsuboi, K.; Sun, Y. X.; Okamoto, Y.; Araki, N.; Tonai, T.; Ueda, N. Molecular characterization of *N*-acylethanolamine-hydrolyzing acid amidase, a novel member of the choloylglycine hydrolase family with structural and functional similarity to acid ceramidase. *J. Biol. Chem.* **2005**, *280*, 11082–11092.

- (22) Zhao, L. Y.; Tsuboi, K.; Okamoto, Y.; Nagahata, S.; Ueda, N. Proteolytic activation and glycosylation of *N*-acylethanolamine-hydrolyzing acid amidase, a lysosomal enzyme involved in the endocannabinoid metabolism. *Biochim. Biophys. Acta* **2007**, *1771*, 1397–1405.

- (23) Wang, J.; Zhao, L. Y.; Uyama, T.; Tsuboi, K.; Tonai, T.; Ueda, N. Amino acid residues crucial in pH regulation and proteolytic activation of *N*-acylethanolamine-hydrolyzing acid amidase. *Biochim. Biophys. Acta* **2008**, *1781*, 710–717.

- (24) Solorzano, C.; Zhu, C.; Battista, N.; Astarita, G.; Lodola, A.; Rivara, S.; Mor, M.; Russo, R.; Maccarrone, M.; Antonietti, F.; Duranti, A.; Tontini, A.; Cuzzocrea, S.; Tarzia, G.; Piomelli, D. Selective *N*-acylethanolamine-hydrolyzing acid amidase inhibition reveals a key role for endogenous palmitoylethanolamide in inflammation. *Proc. Natl. Acad. Sci. U.S.A.* **2009**, *106*, 20966–20971.

- (25) West, J. M.; Zvonok, N.; Whitten, K. M.; Wood, J. T.; Makriyannis, A. Mass spectrometric characterization of human *N*-acylethanolamine-hydrolyzing acid amidase. *J. Proteome Res.* **2012**, *11*, 972–981.

- (26) Lodola, A.; Branduardi, D.; De Vivo, M.; Capoferri, L.; Mor, M.; Piomelli, D.; Cavalli, A. A catalytic mechanism for cysteine *N*-terminal nucleophile hydrolases, as revealed by free energy simulations. *PLoS One* **2012**, *7*, e32397.

- (27) Mor, M.; Rivara, S.; Lodola, A.; Plazzi, P. V.; Tarzia, G.; Duranti, A.; Tontini, A.; Piersanti, G.; Kathuria, S.; Piomelli, D. Cyclohexylcarbamic acid 3'- or 4'-substituted biphenyl-3-yl esters as fatty acid amide hydrolase inhibitors: Synthesis, quantitative structure-activity relationships, and molecular modeling studies. *J. Med. Chem.* **2004**, *47*, 4998–5008.

- (28) Clapper, J. R.; Vacondio, F.; King, A. R.; Duranti, A.; Tontini, A.; Silva, C.; Sanchini, S.; Tarzia, G.; Mor, M.; Piomelli, D. A second generation of carbamate-based fatty acid amide hydrolase inhibitors with improved activity in vivo. *ChemMedChem* **2009**, *4*, 1505–1513.
- (29) Clapper, J. R.; Moreno-Sanz, G.; Russo, R.; Guijarro, A.; Vacondio, F.; Duranti, A.; Tontini, A.; Sanchini, S.; Sciolino, N. R.; Spradley, J. M.; Hohmann, A. G.; Calignano, A.; Mor, M.; Tarzia, G.; Piomelli, D. Anandamide suppresses pain initiation through a peripheral endocannabinoid mechanism. *Nat. Neurosci.* **2010**, *13*, 1265–1270.
- (30) Vandevorde, S.; Tsuboi, K.; Ueda, N.; Jonsson, K.-O.; Fowler, C. J.; Lambert, D. M. Esters, retroesters, and a retroamide of palmitic acid: Pool for the first selective inhibitors of *N*-palmitoylethanolamine-selective acid amidase. *J. Med. Chem.* **2003**, *46*, 4373–4376.
- (31) Tsuboi, K.; Hilligsmann, C.; Vandevorde, S.; Lambert, D. M.; Ueda, N. *N*-Cyclohexanecarbonylpentadecylamine: A selective inhibitor of the acid amidase hydrolysing *N*-acylethanolamines, as a tool to distinguish acid amidase from fatty acid amide hydrolase. *Biochem. J.* **2004**, *379*, 99–106.
- (32) Saturnino, C.; Petrosino, S.; Ligresti, A.; Palladino, C.; De Martino, G.; Bisogno, T.; Di Marzo, V. Synthesis and biological evaluation of new potential inhibitors of *N*-acylethanolamine hydrolyzing acid amidase. *Bioorg. Med. Chem. Lett.* **2010**, *20*, 1210–1213.
- (33) Solorzano, C.; Antonietti, F.; Duranti, A.; Tontini, A.; Rivara, S.; Lodola, A.; Vacondio, F.; Tarzia, G.; Piomelli, D.; Mor, M. Synthesis and structure-activity relationships of *N*-(2-oxo-3-oxetanyl)amides as *N*-acylethanolamine-hydrolyzing acid amidase inhibitors. *J. Med. Chem.* **2010**, *53*, 5770–5781.
- (34) Mayer, R. J.; Louis-Flamberg, P.; Elliott, J. D.; Fisher, M.; Leber, J. Inhibition of 3-hydroxy-3-methylglutaryl coenzyme A synthase by antibiotic 1233A and other β -lactones. *Biochem. Biophys. Res. Commun.* **1990**, *169*, 610–616.
- (35) Lall, M. S.; Karvellas, C.; Vederas, J. C. β -Lactones as a new class of cysteine proteinase inhibitors: Inhibition of hepatitis A virus 3C proteinase by *N*-Cbz-serine β -lactone. *Org. Lett.* **1999**, *1*, 803–806.
- (36) Lall, M. S.; Ramtohl, Y. K.; James, M. N.; Vederas, J. C. Serine and threonine β -lactones: A new class of hepatitis A virus 3C cysteine proteinase inhibitors. *J. Org. Chem.* **2002**, *67*, 1536–1547.
- (37) Arnold, L. D.; Kalantar, T. H.; Vederas, J. C. Conversion of serine to stereochemically pure β -substituted α -amino acids via β -lactones. *J. Am. Chem. Soc.* **1985**, *107*, 7105–7109.
- (38) Baumgarten, H. E.; Smith, H. L.; Staklis, A. Reactions of amines. XVIII. Oxidative rearrangement of amides with lead tetraacetate. *J. Org. Chem.* **1975**, *40*, 3554–3561.
- (39) Bisel, P.; Breitling, E.; Frahm, A. W. Diastereo- and enantioselective synthesis of (+)- and (–)-*cis*-2-aminocyclobutanol. *Eur. J. Org. Chem.*, **1998**, 729–733.
- (40) Arnold, L. D.; May, R. G.; Vederas, J. C. Synthesis of optically pure α -amino acids via salts of α -amino- β -propiolactone. *J. Am. Chem. Soc.* **1988**, *110*, 2237–2241.
- (41) Martinez, E. R.; Salmassian, E. K.; Lau, T. T.; Gutierrez, C. G. Enterobactin and enantioenterobactin. *J. Org. Chem.* **1996**, *61*, 3548–3550.
- (42) Kucharczyk, N.; Badet, B.; Le Goffic, F. Quantitative synthesis of *L*- and *D*-*N*²-(*tert*-butoxycarbonyl)-2,3-diaminopropanoic acid from protected *L*- and *D*-serine β -lactone. *Synth. Commun.* **1989**, *19*, 1603–1609.
- (43) Valls, N.; Borregán, M.; Bonjoch, J. Synthesis of β -chloro α -amino acids: (2*S*,3*R*)- and (2*S*,3*S*)-3-chloroleucine. *Tetrahedron Lett.* **2006**, *47*, 3701–3705.
- (44) Higashibayashi, S.; Kohno, M.; Goto, T.; Suzuki, K.; Mori, T.; Hashimoto, K.; Nakata, M. Synthetic studies on thiostrepton family of peptide antibiotics: Synthesis of the pentapeptide segment containing dihydroxyisoleucine, thiazoline and dehydroamino acid. *Tetrahedron Lett.* **2004**, *45*, 3707–3712.
- (45) Merrifield, R. B. Competitive inhibition of a streptogenin-active peptide by related peptides. *J. Biol. Chem.* **1958**, *232*, 43–54.
- (46) Plattner, Pl. A.; Boller, A.; Frick, H.; Fürst, A.; Hegedüs, B.; Kirchensteiner, H.; Majnoni, St.; Schläpfer, R.; Spiegelberg, H. Syntheses of 4-amino-3-isoxazolidinone (cycloserine) and some analogs. *Helv. Chim. Acta* **1957**, *40*, 1531–1532.
- (47) Hofmann, K.; Schmiechen, R.; Wells, R. D.; Wolman, Y.; Yanaiharu, N. Studies on Polypeptides. XXIX. Synthetic peptides related to the N-terminus of bovine pancreatic ribonuclease A (Position 1–7). *J. Am. Chem. Soc.* **1965**, *87*, 611–619.
- (48) Miller, M. J.; Mattingly, P. G.; Morrison, M. A.; Kerwin, J. F., Jr. Synthesis of β -lactams from substituted hydroxamic acids. *J. Am. Chem. Soc.* **1980**, *102*, 7026–7032.
- (49) Arold, H.; Fischer, V.; Feist, H. Peptides. XI. Synthesis of the heptapeptide with modified potential circulin B-sequence. *J. Prakt. Chem./Chem.-Ztg.* **1969**, *311*, 490–496.
- (50) Shao, H.; Goodman, M. An enantiomer synthesis of *allo*-threonines and β -hydroxyvalines. *J. Org. Chem.* **1996**, *61*, 2582–2583.
- (51) Cohen, S. B.; Halcomb, R. L. Application of serine- and threonine-derived cyclic sulfamidates for the preparation of *S*-linked glycosyl amino acids in solution- and solid-phase peptide synthesis. *J. Am. Chem. Soc.* **2002**, *124*, 2534–2543.
- (52) Gérard, S.; Dive, G.; Clamot, B.; Touillaux, R.; Marchand-Brynaert, J. Synthesis, hydrolysis, azetichemical and theoretical evaluation of 1,4-bis(alkoxycarbonyl)azetid-2-ones as potential elastase inhibitors. *Tetrahedron* **2002**, *58*, 2423–2433.
- (53) Arnold, L. D.; Drover, J. C. G.; Vederas, J. C. Conversion of serine β -lactones to chiral α -amino acids by copper-containing organolithium and organomagnesium reagents. *J. Am. Chem. Soc.* **1987**, *109*, 4649–4659.
- (54) Tove, S. B. The esterolytic activity of serum albumin. *Biochim. Biophys. Acta* **1962**, *57*, 230–235.
- (55) Sakurai, Y.; Ma, S.-F.; Watanabe, H.; Yamaotsu, N.; Hirono, S.; Kurono, Y.; Kragh-Hansen, U.; Otagiri, M. Esterase-like activity of serum albumin: Characterization of its structural chemistry using *p*-nitrophenyl esters as substrates. *Pharm. Res.* **2004**, *21*, 285–292.
- (56) Testa, B.; Mayer, J. M. In *Hydrolysis in drug and prodrug metabolism. Chemistry, biochemistry and enzymology*; Verlag Helvetica Chimica Acta: Zurich, 2003; pp 12–46, 391–393, 477–481.
- (57) Liederer, B. M.; Borchardt, R. T. Enzymes involved in the bioconversion of ester-based prodrugs. *J. Pharm. Sci.* **2006**, *95*, 1177–1195.
- (58) Erdős, E. G.; Boggs, L. E. Hydrolysis of paraoxon in mammalian blood. *Nature* **1961**, *190*, 716–717.
- (59) Gan, K. N.; Smolen, A.; Eckerson, H. W.; La Du, B. N. Purification of human serum paraoxonase/arylesterase. Evidence for one esterase catalyzing both activities. *Drug Metab. Dispos.* **1991**, *19*, 100–106.
- (60) La Du, B. N. Structural and functional diversity of paraoxonases. *Nat. Med.* **1996**, *2*, 1186–1187.
- (61) Kelso, G. J.; Stuart, W. D.; Richter, R. J.; Furlong, C. E.; Jordan-Starck, T. C.; Harmony, J. A. K. Apolipoprotein J is associated with paraoxonase in human plasma. *Biochemistry* **1994**, *33*, 832–839.
- (62) Kuo, C. L.; La Du, B. N. Calcium binding by human and rabbit serum paraoxonases. Structural stability and enzymatic activity. *Drug Metab. Dispos.* **1998**, *26*, 653–660.
- (63) Brandt, E.; Heymann, E.; Mentlein, R. Selective inhibition of rat liver carboxylesterases by various organophosphorus diesters *in vivo* and *in vitro*. *Biochem. Pharmacol.* **1980**, *29*, 1927–1931.
- (64) Turini, P.; Kurooka, S.; Steer, M.; Corbascio, A. N.; Singer, T. P. The action of phenylmethylsulfonyl fluoride on human acetylcholinesterase, chymotrypsin and trypsin. *J. Pharmacol. Exp. Ther.* **1969**, *167*, 98–104.
- (65) Li, B.; Sedlacek, M.; Manoharan, I.; Boopathy, R.; Duysen, E. G.; Masson, P.; Lockridge, O. Butyrylcholinesterase, paraoxonase, and albumin esterase, but not carboxylesterase, are present in human plasma. *Biochem. Pharmacol.* **2005**, *70*, 1673–1684.
- (66) Biggadike, K.; Angell, R. M.; Burgess, C. M.; Farrell, R. M.; Hancock, A. P.; Harker, A. J.; Irving, W. R.; Ioannou, C.; Procopiou, P. A.; Shaw, R. E.; Solanke, Y. E.; Singh, O. M. P.; Snowden, M. A.; Stubbs, R. J.; Walton, S.; Weston, H. E. Selective plasma hydrolysis of glucocorticoid γ -lactones and cyclic carbonates by the enzyme

paraoxonase: An ideal plasma inactivation mechanism. *J. Med. Chem.* **2000**, *43*, 19–21.

(67) Bodor, N. Designing safer drugs based on the soft drug approach. *Trends Pharmacol. Sci.* **1982**, *3*, 53–56.

(68) Druzgala, P.; Hochhaus, G.; Bodor, N. Soft drugs. 10. Blanching activity and receptor binding affinity of a new type of glucocorticoid: Loteprednol etabonate. *J. Steroid Biochem. Mol. Biol.* **1991**, *38*, 149–154.

(69) Moodley, I.; Grouhel, A.; Lelievre, V.; Junien, J. L. Anti-inflammatory properties of tixocortol 17-butyrate,21-propionate (JO 1222), a novel, locally acting corticosteroid. *J. Lipid Mediators* **1991**, *3*, 51–70.

(70) Kwon, T.; Heiman, A. S.; Oriaku, E. T.; Yoon, K.; Lee, H. J. New steroidal antiinflammatory antedugs: Steroidal [16 α ,17 α -d]-3'-carbethoxyisoxazolines. *J. Med. Chem.* **1995**, *38*, 1048–1051.

(71) Zhang, Y.-K.; Plattner, J. J.; Akama, T.; Baker, S. J.; Hernandez, V. S.; Sanders, V.; Freund, Y.; Kimura, R.; Bu, W.; Hold, K. M.; Lu, X.-S. Design and synthesis of boron-containing PDE4 inhibitors using soft-drug strategy for potential dermatologic anti-inflammatory application. *Bioorg. Med. Chem. Lett.* **2010**, *20*, 2270–2274.

(72) Kemeny, L.; Koreck, A.; Kis, K.; Kenderessy-Szabo, A.; Bodai, L.; Cimpean, A.; Paunescu, V.; Raica, M.; Ghyczy, M. Endogenous phospholipid metabolite containing topical product inhibits ultraviolet light-induced inflammation and DNA damage in human skin. *Skin Pharmacol. Physiol.* **2007**, *20*, 155–161.

(73) Ponzano, S.; Bertozzi, F.; Mengatto, L.; Dionisi, M.; Berteotti, A.; Fiorelli, C.; Tarozzo, G.; Reggiani, A.; Tarzia, G.; Mor, M.; Cavalli, A.; Piomelli, D.; Bandiera, T. Synthesis and Structure Activity Relationship (SAR) of 2-methyl-4-oxo-3-oxetanyl carbamic acid esters, a potent class of N-acylethanolamine acid amidase (NAAA) inhibitors. Unpublished results.

(74) Vacondio, F.; Silva, C.; Lodola, A.; Carmi, C.; Rivara, S.; Duranti, A.; Tontini, A.; Sanchini, S.; Clapper, J. R.; Piomelli, D.; Tarzia, G.; Mor, M. Biphenyl-3-yl alkylcarbamates as fatty acid amide hydrolase (FAAH) inhibitors: Steric effects of N-alkyl chain on rat plasma and liver stability. *Eur. J. Med. Chem.* **2011**, *46*, 4466–4473.

(75) *Maestro*, version 9.0; Schrodinger, LLC: New York, 2009.

(76) Par, R. G.; Yang, W. *Density-functional theory of atoms and molecules*; Oxford University Press: Oxford, U.K., 1989.

(77) *Jaguar*, version 7.6; Schrodinger, LLC: New York, 2009.

(78) Becke, A. D. Density-functional thermochemistry. III. The role of exact exchange. *J. Chem. Phys.* **1993**, *98*, 5648–5652.